Organic & Supramolecular Chemistry

Nano-Manufacturing Supramolecular Structures of Bio-Inspired Naphthalene Diimide Bolaamphiphile *via* Solvophobic Controlled Self-Assembly

Santosh P. Goskulwad,[a, b] Duong Duc La,[c] Rajesh S. Bhosale,[a] Mohammad Al Kobaisi,[b] Lathe A Jones,[c] Sidhanath V. Bhosale,*[a, b] and Sheshanath V. Bhosale*[c, d]

We report the synthesis of a naphthalene diimide bolaamphiphile (**NDI-1**) bearing the peptide segment of Tyr-Glu and studied self-assembly through solvophobic control. **NDI-1** is shown to self-assemble into a flower-like morphology from its 4:6 THF/methylcyclohexane (MCH) (*v/v*) solution. Microscale broad grass-like structures were obtained from **NDI-1** solution in 2:8 THF/H_2O (*v/v*). The assembly formation was visualised by scanning electron microscope (SEM) imaging, furthermore, XRD used to determined mode of aggregation. This work demonstrates that complex self-assembly can indeed be attained through hierarchical non-covalent interactions of bio-inspired naphthalene diimide-peptide conjugates.

Introduction

In nature self-assembly is a ubiquitous process, which plays an important role in the formation of functional, complex biological nanoscale structures.[1] The self-assembly process is responsible for functional machinery of life such as ion channels, the photosynthetic system, and catalysis in enzymatic pockets.[2] Molecular recognition and specific interactions at the molecular level result in a variety of self-assembled structures such as nucleic acids, proteins, cell membranes, collagens and viruses.[3] Nature provides biomolecular building blocks of precise shape and size for biological self-assembly. Inspired by the bottom-up materials self-assembly in nature, scientists have employed the principles used by nature to fabricate functional artificial materials to self-assemble *via* non-covalent interactions such as hydrogen bonding, π-π, hydrophobic, van der Waals and electrostatic interactions using biological and synthetic building blocks.[4] Intrestingly, Bag and co-workers reported the complex flower-like architecrutres from spontaneous self-assembly of a few natural products such as Betulin, triterpenoid 18β-glycyrrhetinic acid without structural modifications.[5] The self-assembly of such building blocks are dynamic. The shape and size of such supramolecular self-assemblies depend upon the molecular structure of the building blocks, which provide precise intra- and intermolecular interactions. In the design of different building blocks to fabricate nanomaterials *via* non-covalent interactions, a high degree of directionality in the self-assembly process is required.[6] This can provide a versatile platform for the fabrication of functional materials with high level of precision and complexity. Though supramolecular chemistry has improved our ability to achieve functions such as molecular recognition, ion transport, catalysis, adaptation and stimuli responsiveness, the field is still in its infancy in some respects. For example, controlling supramolecular nanostructures of π-conjugated system that emerge through non-covalent interactions is still a challenging task.

Naphthalene diimide (NDI) is aromatic π-conjugated planar molecule, which exibits high π-acidity leading to face-to-face π-stacking in self-assembly processes. Functionalised NDIs have been widely used as important bulding blocks for fabrictaion of functional supramolecular nanomaterials, with applications in various fields such as organic field effect transistors, organic photovoltaics, supramolecular switches, artificial photosystems, catalysis, chemosensors, biosensors and the degradation of pollutants.[7] Various organised structures such as nanotubes, nanospheres, fractals, golf-ball like morphologies, nanoflowers, vesicles, nanowires and nanobelts have been successfully fabricated from chemically modified NDI derivatives.[8] Although some 3D complex morphologies of NDI assemblies have been achieved, understanding how to precisely control the assembly of complex nanostructure materials remains a challenging task. This issue can only be overcome by advances in molecular design, and the improvement of the solubility of NDIs in various solvents. In this regard, subunit peptide conjugation to the imide of NDI results in promising candidates, with the capability of tunable, complex self-organisation.[9]

In this work, we utilised peptide appended NDI to induce and manipulate the self-assembly behaviour, where the peptide

[a] S. P. Goskulwad, Dr. R. S. Bhosale, Dr. S. V. Bhosale
      Polymers and Functional Materials Division, CSIR-Indian Institute of Chemical Technology, Hyderabad 500007, Telangana, India
      E-mail: bsheshsnath@gmail.com
[b] S. P. Goskulwad, Dr. M. A. Kobaisi, Dr. S. V. Bhosale
      Academy of Scientific and Innovative Research (AcSIR), CSIR-IICT, Hyderabad 500007, Telangana, India
      E-mail: bhosale@iict.res.in
[c] Dr. D. D. La, Dr. L. A. Jones, Dr. S. V. Bhosale
      School of Science, RMIT University, GPO Box 2476, Melbourne VIC- 3001
[d] Dr. S. V. Bhosale
      Department of Chemistry, Goa University, Taleigo Plateau, Goa-403206, India
      E-mail: bsheshanath@unigoa.ac.in

Supporting information for this article is available on the WWW under https://doi.org/10.1002/slct.201702934

subunit was simply substituted at the imide position of NDI. The integration of NDI and the peptide (Tyr-Glu) offered a new possibility of self-assembly to fabricate flower-like micro-architectures, with the opportunity to tune these structures with changes in the solvent systems.

Results and Discussion

Here we present micron size flowers of **NDI-1**, composed of petals of nanometer dimensions. The design of **NDI-1** is based on our recent results in which we showed the asymmetric NDI amphiphile bearing L-phenyl alanine subunit conjugated to glutamate self-assembled into golf-ball like nanostructures. In continuation of our work we replaced L-phenylalanine with L-tyrosine and invested their self-assembly.[8d] The self-assembly process and flower like morphology is characterized using UV-vis, fluorescence emission spectroscopy and X-ray diffraction, and visualized by scanning electron microscopy, and polarised microscopy.
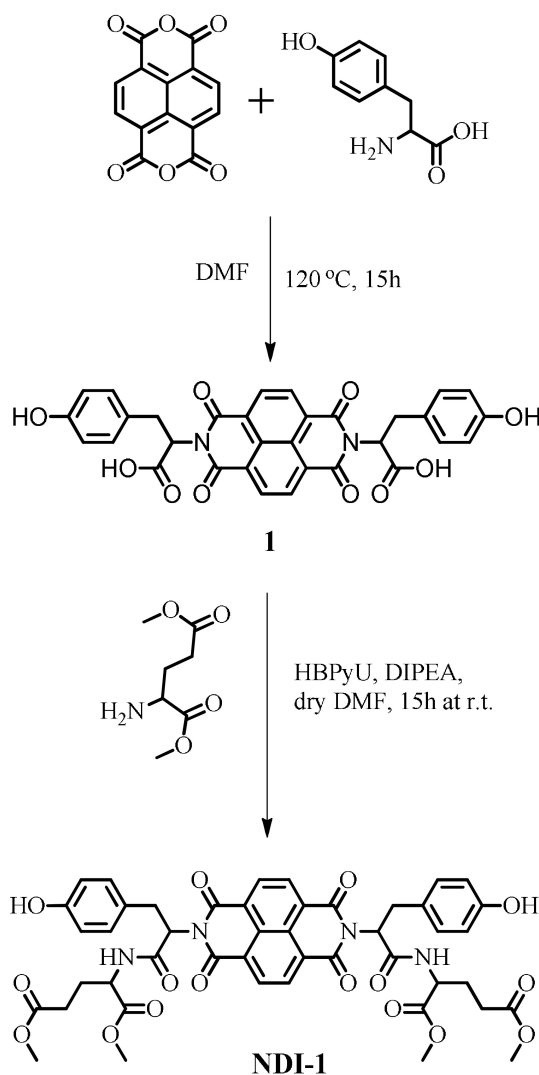
Synthesis of NDI-1

The bolaamphiphile **NDI-1** (Scheme 1) was synthesised, purified and characterized according to a reported procedure.[10] Bolaamphiphile **NDI-1** was further reacted with glutamate via an amide coupling reaction to yield the more hydrophobic naphthalene diimide bolaamphiphile **NDI-1,** and characterized by FT-IR, ^{1}H NMR, ^{13}C NMR, ESI-mass and HRMS spectroscopy techniques (Figure S1-S5, ESI†).

Thermogravimetric (TGA) and differential scanning calorimetry (DSC) experiments were employed to study the thermal properties of **NDI-1. NDI-1**, 2% weight loss temperature (T_d) was observed at 266.26 °C (Figure S6), suggests good stability. DSC of **NDI-1** (Figure S7) shows 215.62 °C and 233.89 °C melting temperatures (T_m) confirming the thermal stability obtained via TGA.

Scheme 1. Synthetic pathway for naphthalene diimide bolaamphiphile **NDI-1**.

UV-vis and fluorescence study

NDI-1 is well solvated in a good solvent such as THF, while sparingly soluble in MCH (nonpolar) and H_2O (polar), indicating that the self-assembly of **NDI-1** can controlled by varying the ratio of these good and bad solvents in solvent mixtures. As such, the self-assembly of **NDI-1** was first investigated in THF upon incremental addition of MCH.

UV-vis absorption spectroscopy was first employed to investigate the aggregation of **NDI-1** from its monomeric state to an aggregated state by varying the MCH/THF volumetric ratio. The concentration of **NDI-1** was fixed at 1×10^{-5} M. The characteristic UV-vis absorption bands appeared in the range of 300–400 nm, attributed to the π-π* transitions in the NDI backbone (Figure 1a). **NDI-1** exhibits absorption bands at 360 nm and 380 nm, along with a shoulder peak at 342 nm in pure THF, indicating the presence of **NDI-1** in monomeric form. Upon incremental addition of MCH to THF, a decrease in peak intensities was observed. At MCH 90 vol% in THF:MCH solvent composition, the absorption peak of **NDI-1** at 380 nm becomes broad and peaks at 342 nm and 360 nm were unaffected. Thus, the decrease in intensity and minimal bathochromic shift of the absorption band indicates aggregation in **NDI-1** self-assembled process. We then investigated the aggregation behaviour of **NDI-1** upon incremental addition of H_2O to THF solution using UV-vis absorption spectroscopy. The peaks at 342, 360 and 380 nm bathochromic shifted to 344, 364 and 385 nm, respectively (Figure 1b). The decrease in UV-vis absorption peak intensity in THF: H_2O (Figure 1b) implies the low solubility of **NDI-1** in more polar conditions with increasing f_w in THF/water solvent compositin, indicating aggregate formation. The self-assembled aggregate formation would be due to repulsive interaction between aromatic NDI core and polar solvent water as well as the π-π stacking interaction between the NDI core. It is reported that water molecule possess lower energy state in bulk water in comparison to water solvating aromatic molecules.[11] The reduced exposure of the aromatic surface to the water enhances the π-π stacking interactions.
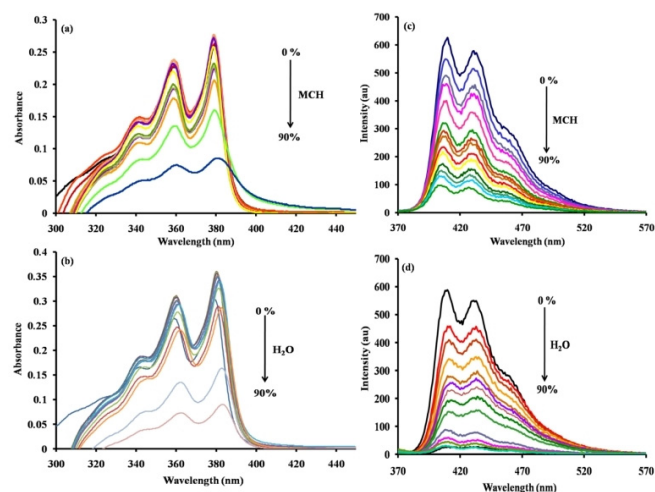
Figure 1. UV-Vis spectra of **NDI-1** (1×10^{-5} M) in (a) THF and THF/MCH in various ratios of MCH (0–90%); (b) THF and THF/H$_2$O in various rations of H$_2$O (0–90%). Fluorescence emission spectra of **NDI-1** (1×10^{-5} M) in (c) THF and THF/MCH in various ratios of MCH (0–90%) (d) THF and THF/H$_2$O in various ratios of H$_2$O (0–90%) at room temperature. Arrows in Figure a, b, c and d indicates the change in absorption and fluorescence intensity upon increasing the percentage of MCH and H$_2$O in THF, respectively.

Figure 2. (a) Field emission electron micrographs (FE-SEM) of the 3D hierarchical flower-like structures of **NDI-1** (1×10^{-5} M). These aggregate formed from 4:6 THF/MCH (*v/v*); (b and c) A zoomed image of flower; (d) Flower consists of petals of nanometre dimensions.

To gain further insight into self-assembled aggregates of **NDI-1**, we carried out fluorescence emission spectroscopy in THF solution (1×10^{-5} M) upon excitation at $\lambda_{ex} = 360$ nm, which gave two prominent peaks at 410 and 431 nm (Figure 1c). The solvent dependent fluorescence of **NDI-1** was investigated with incremental addition of nonpolar MCH in a THF solution of **NDI-1** leading to a decrease in peak intensities at 410 and 431 nm respectively. This indicates π-π stacking of the NDI core leading to fluorescence quenching. Similar behaviour was observed with the addition of a polar solvent such as water into a solution of **NDI-1** in THF, which led to a significant decrease in peak intensities at 410 and 431 nm (Figure 1d). From fluorescence emission results it is clear that at a higher MCH and water content in THF solution, **NDI-1** undergoes aggregation *via* π-π stacking.

Morphology study of NDI-1

Scanning electron microscopy (SEM), polarized optical microscopy (POM), dynamic light scattering (DLS) and x-ray diffraction (XRD) studies were also employed to investigate the morphology obtained *via* self-assembly of **NDI-1.**

Scanning electron microscopy study

Self-assembled nanostructures of **NDI-1** were prepared by slow evaporation of THF:MCH solutions onto a Silicon wafer at room temperature, followed by drying under vacuum in a desiccator. The images of the objects obtained from FE-SEM are shown in Figure 2a-d. The self-assemblies of **NDI-1** prepared from the THF:MCH solution (4:6, *v/v*) showed complex 3D flower-like
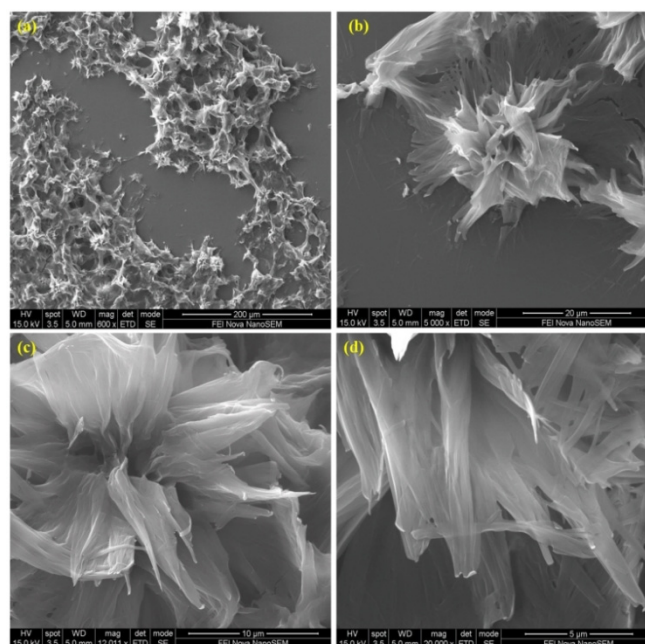
superstructures. As shown in Figure 2a-c, the flower-like microstructures are of 10–15 μm diameters.

The flower-like assemblies of **NDI-1** obtained from THF:MCH are comprised of dozens of petals (2D sheets) (Figure 2d). These petals are produced by growth from a common centre. The petal-like building subunits are revealed to be several micrometers long and composed of 200–400 nm wide strips. This obtained morphology is formed from aggregatation, as suggested by absorption spectroscopy results, which is based on the inter- and intra molecular hydrogen bonding, hydrophobic, π-π stacking and solvophobic interactions. The hydrogen bonding between the hydroxyl head groups of **NDI-1**, amide hydrogen bonding, along with π-π stacking of NDI core in cooperation with solvent interaction yields the flower-like morphology.

Furthermore, the role of varying THF:MCH solvents ratio on **NDI-1** supramolecular organization was examined by conducting FE-SEM microscopy of samples deposited from a THF:MCH 2:8 (*v/v*) solution (Figure S8a-b). Highly polydispersed and uniform 2D nanoplates structures with a size distribution of several micrometers in length and width are formed under these experimental conditions. As shown in Figure S8c, the nanoplates are formed by a disordered-aggregation of nanosheets that are several nanometers in diameter. As shown in the SEM images, 3D flower-like morphology (THF:MCH 2:8, *v/v*) and 2D nanoplates (THF:MCH 4:6, *v/v*) was clearly observed, these results suggests that f_{MCH} plays an important role in the aggregation process. The effect of polarity was investigated for NDI-1 in THF:MCH with different compositions such as 4:6 and 2:8 vol%. In pure THF solvent, **NDI-1** is in monomeric form.

Upon addition of nonpolar solvent MCH, the NDI-1 undergoes aggregation via non-covalent interactions such as amide H-bonding, π-π stacking. The solubility of **NDI-1** in THF:MCH goes on decreasing with increasing in f_{MCH}. At THF:MCH 4:6 vol% solvent composition, **NDI-1** undergoes initially in dimer formation (Figure 6) which leads to petals (Figure 2D) which in turn converted into 3D-flower-like assembly. With further increase in f_{MCH} i.e. THF:MCH 2:8 vol%, we presume that due to high nonpolar MCH fraction, repulsive interactions of aromatic NDI core with nonpolar solvent as well as increase in π-π stacking resulted into more aggregated 2D-nanoplates. These nanostructures can be prepared with great reproducibility when solvent mixtures and evaporation process are carefully controlled.

The effect of solvent polarity on the **NDI-1** self-assembly process was explored in THF:water solutions of at various ratios. **NDI-1** supramolecular self-assemblies were deposited from solutions in THF:water at 2:8 and 4:6 (v/v) ratios. A broad grass-like supramolecular nanostructures were produced by drop casting of **NDI-1** solution in THF:water (2:8, *v/v*) onto Silicon wafer surfaces (Figure 3a-d) at room temperature. These grass-
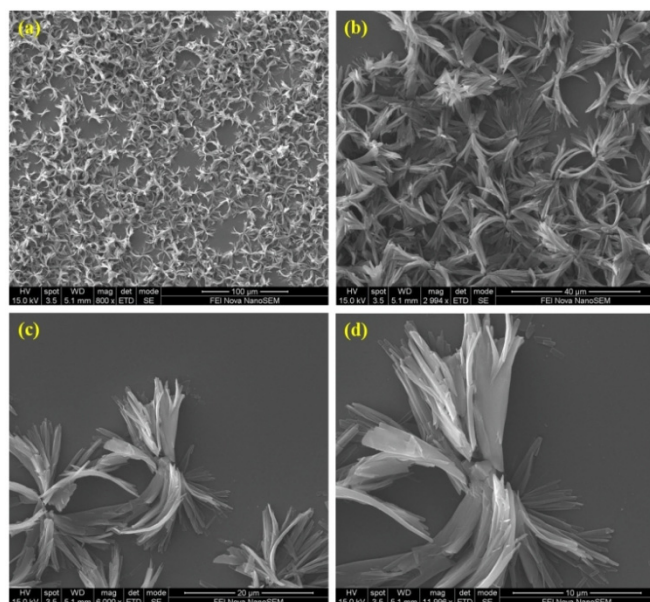

Figure 3. SEM images of self-assemblies formed by **NDI-1** (1×10^{-5} M) in 2:8 THF/H_2O (*v/v*) ratio. (a, b) formed windows grill like fibril networks; (c, d) depict zoomed images of fibril networks morphology 20 and 10 μm scale, respectively.

like microstructures were highly uniform with an average length of 10 μm. These grass-like formations are composed of stacking of smaller and thinner 5–10 μm in length and tens of nanometres in width sheets as shown in Figure 3c-d.

At lower water ratio results in higher solubility of **NDI-1**. Figure S9a-b shows FE-SEM micrographs of deposited **NDI-1** from THF:water (4:6, v/v) solution with large non-crystalline solid alongside smaller sheet-like structures. The lower level of self-assembly observed at higher THF ratios in THF:water

solvent mixture can be due to the higher solubility and reduced solvophobic effects and thus less nucleation in the stock solution prior solvent evaporation and solid deposition on the substrate. At higher THF ratio the hydrophobic moieties of the **NDI-1** molecular structures are better solvated, resulting in reduced intermolecular π-π interaction between the NDI core and hydrophobic interaction between glutamates essential to form the aggregates. Thus, one can control the morphology of the produced supramolecular structures resulting from self-assembly by simply controlling the experimental conditions such as the solvent ratio water in THF.

Dynamic light scattering

The solvophobic effect on the self-assembly in solution confirms the formation of the nuclei of supramolecular micro-structures in solution prior to growth and formation on the substrate due to solvent evaporation was also studied using dynamic light scattering (DLS). The hydrodynamic diameter of **NDI-1** self-assemblies in solution in THF:MCH (4:6 and 2:8, *v/v*) (Figure S10) and THF:water (4:6 and 2:8, *v/v*) (Figure S11) were further investigated by DLS. In THF:MCH (4:6, *v/v*) 71.9% of assemblies of **NDI-1** had an average diameter of 300 nm. At higher MCH ratio with more solvophobic effect, THF:MCH (2:8, *v/v*), 100% of assemblies hydrodynamic diameter increased to an average of 550 nm. Similarly at higher water ratio with more solvophobic effect, in THF:H_2O (2:8, *v/v*) the average hydrodynamic diameters was 362 nm, while with increased THF and increased solvation of **NDI-1** molecules, at THF:water (4:6, *v/v*), 100% of self-assemblies in solution were reduced to 304 nm in hydrodynamic diameter.

Polarised optical microscopy

In order to evaluate the self-assembled nanostructures, we examined the morphology of self-assembled **NDI-1** in produced in different solvent mixtures, THF: MCH (4:6, v/v) and THF: water (2:8, v/v), by polarised optical microscopy Figure S12 (a and b). POM images in THF:MCH (4:6, v/v) displays **NDI-1** self-assembled into a globular nano-architecture, it is very hard to clear visulaize, we presume that it could be flower-like aggregates Figure 12S(a). However, POM images in THF: water (2:8, v/v), **NDI-1** shows clear flower-like objects such as present in windows grill Figure S10 (b). Thus, POM images Figure S12 (b) of **NDI-1** clearly reveal formation of windows grill flower like assemblies such as 3D Figure 3a-d.

X-ray diffraction study

Figure 4 shows the XRD patterns of **NDI-1** solids deposited from THF/H_2O and THF/MCH solutions at 4:6 and 2:8 ratios of each. Very weak reflections can be observed at the 60% water and MCH ratios. This is due to the higher solubility of **NDI-1** in these solvent mixtures resulting in highly amorphous solid. Increasing the bad solvents of water and MCH ratios in the solvent mixtures enhances the crystallization process in solution prior to deposition, resulting the intensity of reflec-
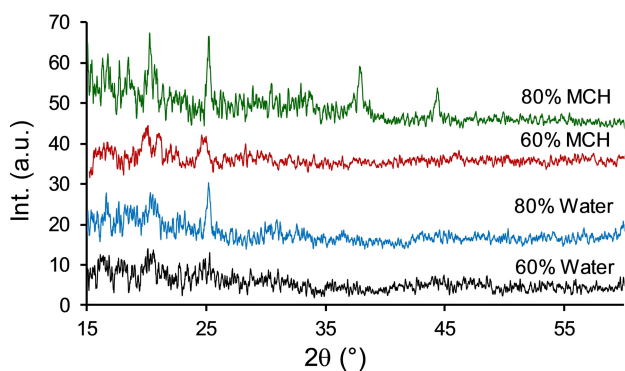
Figure 4. XRD patterns of monomeric **NDI-1** molecule and nanostructures via supramolecular self-assembly of **NDI-1** in various solvent mixtures of THF/H$_2$O (40:60 and 20:80) and THF/MCH (40:60 and 20:80).

tions at 80% ratios of water and MCH. Crystal growth in THF/water is more directional as evidenced by the reflection at 25.3° and the lack of peaks at 37.9° and 44.4°. The appearance of peaks at these two angles shows growth of the self-assembly of **NDI-1** in all possible directions. The non-crystalline nature of **NDI-1** aggregates in a mixture of THF/H$_2$O with water fraction of 60% was also confirmed by the poorly-defined morphology shown in Figure S9. However, the XRD patterns of assembled **NDI-1** in THF/H$_2$O with water fraction of 80%, THF/MCH with MCH fraction of 60% and 80% shows several characteristic of the assembled **NDI-1** microstructures. These results indicate that assembled **NDI-1** aggregates are crystalline in nature.

Density functional theory study

Furthermore, to investigate the electronic structure of **NDI-1**, time dependent density functional theory (TDDFT) calculations were carried out. The *in vacuo* TDDFT calculations using the Gaussian 16 suit of programs[12] and the B3LYP/6-311+G(d,p) level of theory of **NDI-1** gave a HOMO-LUMO gap of 542.5 nm (2.29 eV) (Figure 5). Table S1 list the first 15 singlet excitations
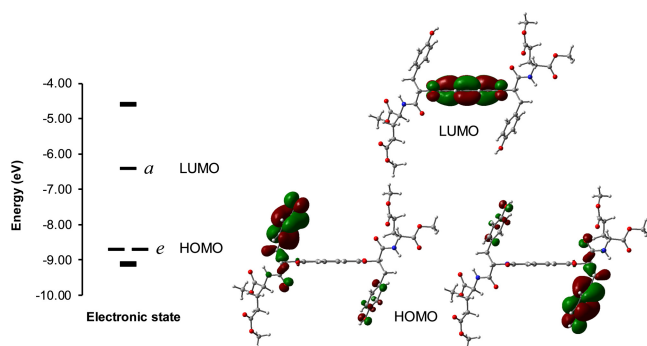

Figure 5. The frontier molecular orbitals HOMO and LUMO wave function and energy levels of **NDI-1** as calculated at B3LYP/6-311+G(d,p) level of theory.

of the **NDI-1** molecule, which are in agreement with its absorption and the emission spectra

Schematic presentation of assembly

The molecular conformation also indicates intermolecular π-π stacking and H-bonding interaction. Figure 6 shows a sche-
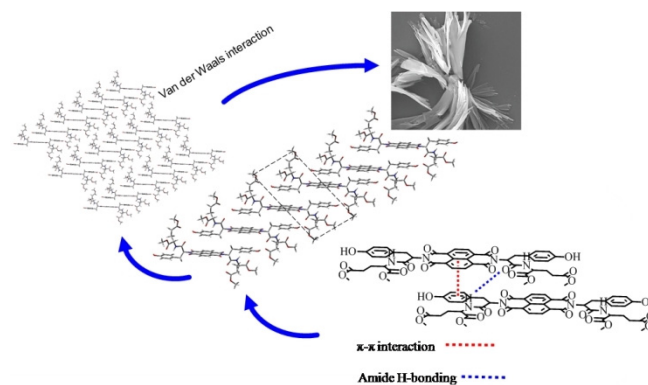

Figure 6. Plausible self-assembly of **NDI-1** to give the petals of the flower like superstructure.

matic presentation of the aggregation mode of **NDI-1** self-assembly giving a sheet supramolecular structure, which can stack to form petals of the flower-like and grass-like supramolecular self-assemblies.

These self-assemblies of **NDI-1** are driven by the intermolecular amide hydrogen bonding and the π-π stacking interactions between the aromatic NDI cores and phenyl moieties resulting in stack self-assemblies (Figure 6). The large N-substitutions in **NDI-1** result in a slight twist in the molecular structure which can be further transferred to the supramolecular self-assembled sheets preventing large scale crystallization and carrying the twist to the sheets geometry which can result in a fractal growth and the formation of the flower-like super structure

Conclusions

In summary, a novel NDI bolaamphiphile i.e. naphthalene diimide substituted with peptide conjugate (**NDI-1**) small molecule, was synthesized, furthermore, we have developed a simple method to fabricate flower–like superstructure self-assemblies. The **NDI-1** micro-flower self-assembly grown from THF:MCH solution, while **NDI-1** in THF: H$_2$O solution resulted in broad grass-like morphology. We assume that the development of such peptide-incorporated micro-flowers of naphthalene diimides may have potential applications in material chemistry.

Supporting Information Summary

Supporting information includes experimental procedures for synthesis of **NDI-1**, procedure for self-assembly, UV-vis,

fluorescence, SEM and POM measurements, the FT-IR, ^{1}H NMR, ^{13}C NMR, mass and HRMS spectras, TGA, DSC, DLS, SEM and POM images and TD-DFT calculations.

Conflict of Interest

The authors declare no conflict of interest.

[1] a) G. Whitesides, J. Mathias, C. Seto, *Science* **1991**, *254*, 1312–1319; b) G. M. Whitesides, B. Grzybowski, *Science* **2002**, *295*, 2418–2421; c) B. A. Grzybowski, C. E. Wilmer, J. Kim, K. P. Browne, K. J. Bishop, *Soft Matter* **2009**, *5*, 1110–1128.

[2] a) M. R. Banghart, M. Volgraf, D. Trauner, *Biochemistry* **2006**, *45*, 15129–15141; b) B. Hille, C. M. Armstrong, R. MacKinnon, *Nat. Med.* **1999**, *5*, 1105–1109; c) J. Barber, P. D. Tran, *J. R. Soc. Interface* **2013**, *10*, 20120984; d) G. M. Cooper, D. Ganem, *Nat. Med.* **1997**, *3*, 1042–1042.

[3] a) S. Zhang, *Mater. Today* **2003**, *6*, 20–27; b) S. Zhang, *Nat. Biotechnol.* 2003, *21*, 1171–1178; c) C. A. Hauser, S. Zhang, *Nature* **2010**, *468*, 516–517; d) N. Amdursky, M. Molotskii, E. Gazit, G. Rosenman, *J. Am. Chem. Soc.* **2010**, *132*, 15632–15636; e) E. Busseron, Y. Ruff, E. Moulin, N. Giuseppone, *Nanoscale* **2013**, *5*, 7098–7140; f) C. Rest, R. Kandanelli, G. Fernández, *Chem. Soc. Rev.* **2015**, *44*, 2543–2572; g) J.-M. Lehn, *Supramolecular chemistry, Vol. 1*, Vch, Weinheim, **1995**.

[4] D. Philp, J. F. Stoddart, *Angew. Chem. Int. Ed.* **1996**, *35*, 1154–1196.

[5] a) B. G. Bag, S. S. Dash, *Langmuir* **2015**, *31*, 13664–13672; b) B. G. Bag, R. Majumdar, *RSC Adv.* **2012**, *2*, 8623–8626; c) B. G. Bag, R. Majumdar, *Chem. Rec.* **2017**, *17*, 841–873.

[6] a) F. J. Hoeben, P. Jonkheijm, E. Meijer, A. P. Schenning, *Chem. Rev.* **2005**, *105*, 1491–1546; b) J. W. Steed, D. R. Turner, K. Wallace, *Core concepts in supramolecular chemistry and nanochemistry*, John Wiley & Sons, **2007**.

[7] a) M. A. Kobaisi, S. V. Bhosale, K. Latham, A. M. Raynor, S. V. Bhosale, *Chem. Rev.* **2016**, *116*, 11685–11796; b) S. V. Bhosale, C. H. Jani, S. J. Langford, *Chem. Soc. Rev.* **2008**, *37*, 331–342; c) C. Röger, F. Würthner, *J. Org. Chem.* **2007**, *72*, 8070–8075; d) B. A. Jones, A. Facchetti, M. R. Wasielewski, T. J. Marks, *J. Am. Chem. Soc.* **2007**, *129*, 15259–15278; e) S. V. Bhosale, S. V. Bhosale, M. B. Kalyankar, S. J. Langford, *Org. Lett.* **2009**, *11*, 5418–5421; f) J. G. Laquindanum, H. E. Katz, A. Dodabalapur, A. J. Lovinger, *J. Am. Chem. Soc.* **1996**, *118*, 11331–11332; g) E. B. Namdas, I. D. Samuel, D. Shukla, D. M. Meyer, Y. Sun, B. B. Hsu, D. Moses, A. J. Heeger, *Appl. Phys. Lett.* **2010**, *96*, 11.

[8] a) G. D. Pantoş, J. L. Wietor, J. K. Sanders, *Angew. Chem. Int. Ed.* **2007**, *46*, 2238–2240; b) M. Tomasulo, D. M. Naistat, A. J. White, D. J. Williams, F. M. Raymo, *Tetrahedron Lett.* **2005**, *46*, 5695–5698; c) H. Shao, T. Nguyen, N. C. Romano, D. A. Modarelli, J. R. Parquette, *J. Am. Chem. Soc.* **2009**, *131*, 16374–16376; d) S. P. Goskulwad, D. D. La, R. S. Bhosale, M. Al Kobaisi, S. V. Bhosale, S. V. Bhosale, *RSC Adv.* **2016**, *6*, 39392–39395; e) N. V. Ghule, D. D. La, R. S. Bhosale, M. Al Kobaisi, A. M. Raynor, S. V. Bhosale, S. V. Bhosale, *ChemistryOpen* **2016**, *5*, 157–163; f) K. P. Nandre, S. V. Bhosale, K. R. Krishna, A. Gupta, S. V. Bhosale, *Chem. Commun.* **2013**, *49*, 5444–5446; g.) R. S. Bhosale, M. Al Kobaisi, S. V. Bhosale, S. Bhargava, S. V. Bhosale, *Sci. Rep.* **2015**, *5*, 14609.

[9] a) E. Gazit, *Nat. Chem.* **2010**, *2*, 1010–1011; b) S. Zhang, T. Holmes, C. Lockshin, A. Rich, *Proc. Natl. Acad. Sci. USA* **1993**, *90*, 3334–3338; c) C. Semino, *J. Dent. Res.* **2008**, *87*, 606–616; d) J. H. Collier, J. S. Rudra, J. Z. Gasiorowski, J. P. Jung, *Chem. Soc. Rev.* **2010**, *39*, 3413–3424; e) S. Maude, L. Tai, R. Davies, B. Liu, S. Harris, P. Kocienski, A. Aggeli, in *Peptide-Based Materials*, Springer, **2011**, pp. 27–69; f) S. Hu, J.-H. Cho, D. H. Gracias, in *Three-Dimensional Nanoarchitectures*, Springer, **2011**, pp. 1–28; g) X. Zhao, F. Pan, J. R. Lu, *Prog. Nat. Sci.: Mater. Int.* **2008**, *18*, 653–660; h) S. H. Yoo, H.-S. Lee, *Acc. Chem. Res.* **2017**, *50*, 832–841.

[10] M. Pandeeswar, H. Khare, S. Ramakumar, T. Govindaraju, *RSC Adv.* **2014**, *4*, 20154–20163.

[11] J. Israelachvili, H. Wenneerström, *Nature* **1996**, *379*, 219–225.

[12] Gaussian 16, Revision A.03, M. Frisch, G. Trucks, H. Schlegel, G. Scuseria, M. Robb, J. Cheeseman, G. Scalmani, V. Barone, G. Petersson, H. Nakatsuji, *et al.* Gaussian, *Inc., Wallingford CT*, **2016**.